AIAA JOURNAL
Vol. 40, No. 7, July 2002

Effects of Coflow on Turbulent Flame Puffs

J. C. Hermanson,* R. Sangras,† J. E. Usowicz,‡ and H. Johari§
Worcester Polytechnic Institute, Worcester, Massachusetts 01609

Pulsed, turbulent jet diffusion flames in an air coflow of variable strength were examined experimentally. In all cases, the flames were fully modulated, that is, the fuel flow was completely shut off between pulses. Isolated puffs of unheated ethylene fuel were injected using a 2-mm-diam-nozzle into a combustor with an air coflow at 1-atm pressure. For short injection times ($\tau < 50$ ms), compact, pufflike structures were generated. The mean flame length of these puffs was at least 51% less than that of a steady-state, that is, nonpulsed, flame for the same injection Reynolds number. More elongated flame structures, with a flame length closer to that of steady-state flames, occurred for longer injection times of up to 300 ms. The addition of coflow generally causes an increase in the mean flame length. For short injection times ($\tau < 50$ ms), this resulted in an increase in flame length of up to 27% for a coflow strength of $U_{cof}/U_{jet} = 0.02$. The fractional increase in the flame length due to coflow of pulsed flames with longer injection times, as well as steady flames, was significantly less. The mean flame length for the flame with the coflow duct generally exceeded that of the corresponding free flame, even for the case of zero coflow. The amount of coflow required to achieve a given increase in mean flame length is quantitatively consistent with a scaling argument developed as part of this investigation.

Introduction

PULSED combustion appears to have the potential for high combustion and thermal efficiencies, excellent heat transfer characteristics, and low CO, NO_x, and soot emissions.[1] A significant amount of research on pulse combustors has examined the overall system characteristics, such as heat transfer, efficiency, frequency of operation, and pollutant formation.[2] The complicated nature of this problem, which includes the strong coupling between the combustion processes and the acoustic field and the confinement due to the combustor chamber walls, is, however, an obstacle to achieving an increased understanding of the fundamental fluid mechanical and combustion mechanisms in these flows.

Some pulsed combustor configurations involve the premixing of fuel and air before entering the combustion chamber.[3] In many practical pulsed combustors, however, the fuel and air enter through separate valves, which control the supply of reactants to the combustor.[4] In this case, the turbulent mixing of the distinct fuel stream and airstream is an essential part of the combustion process. One important aspect of these flows is the nature of the large-scale turbulent structures and the implications of those structures for fuel/air mixing and combustion.

The numerous fundamental studies to date of pulsed jet configurations without acoustic coupling effects may be helpful in understanding the fuel/air mixing and combustion processes in pulsed combustion systems. Much of the research conducted in unsteady reacting and nonreacting jet flows to date has involved direct forcing of the jet with a specified acoustic input. In isothermal jets, such forcing has been shown to result in increased spreading rates and in enhanced mixing over unforced jets.[5–7] These studies have shown that noticeable changes in nonreacting jet growth and entrainment can be achieved even at relatively low pulsation frequencies (of the order of 10 Hz). The effects of acoustic forcing have been seen as far downstream as 70 nozzle diameters, with an increase in local entrainment by as much as a factor of three.[8] Turbulent flames have also been seen to be sensitive to acoustic-level pulsing of the fuel stream.[9] Forcing turbulent flames at low frequency (again, approximately 10 Hz) can produce marked changes in the buoyant structure in the far field, with a significant impact on the flame length and fuel/air mixing. Other research involving acoustic excitation or feedback has been conducted with both nonpremixed and premixed flames in ramjets,[10] pulsed combustors,[4,11] and other ducts.[12,13] Each of those combustor configurations is, however, characterized by a strong coupling between the combustion process and the acoustic field.

A fundamentally different approach to unsteady combustion than acoustic forcing is to fully modulate the fuel jet flow, that is, to completely shut off the fuel jet between pulses using an externally controlled valve. This can give rise to drastic modification of the flow characteristics of flames, leading to enhanced fuel/air mixing processes not operative for the case of acoustically excited or partially modulated jets.[14,15] Although full modulation of the flow can be realized in pulsed combustor configurations,[4,16] such pulsing is necessarily accompanied by the very strong acoustic coupling noted earlier, the properties of which (such as frequency) are strongly facility dependent and can be difficult to vary over a wide range without hardware modification.

Experiments on unconfined, fully modulated flames by Johari and Motevalli[14] showed a decrease in mean flame length for the case of widely separated buoyant fuel puffs of up to 70% compared with a steady, that is, nonpulsed, turbulent flame at low Reynolds number ($Re_{jet} \approx 2 \times 10^3$). They examined not only the effects of pulsing frequency on flame length and structure but also those due to the duty cycle, that is, the jet-on fraction of each pulsation cycle. Subsequent work by Hermanson et al.[15] demonstrated a flame length reduction of approximately 50% for Reynolds numbers of up to $Re_{jet} = 2 \times 10^4$. That work also revealed two distinct types of flame structure for fully modulated flames. For short injection times of approximately 35–45 ms for a 6.4-mm-diam nozzle, pufflike flame structures with a roughly spherical shape and a very short flame length were observed. For longer injection times of up to 120 ms, more elongated flames resulted. The flame lengths of the elongated flames were generally comparable to those of the corresponding steady-state cases.

The focus of the current work is the extension of previous research in fully modulated, turbulent, diffusion flames to include the effects of an air coflow of variable strength. The importance of understanding the impact of coflow on fully modulated diffusion flames stems both from the need to be able to conduct experiments in situations in which the flow rate of oxidizer available may be strictly limited (such as on a space platform) and to contribute to the understanding of configuration and confinement effects in pulsed combustion systems.

Received 13 March 2001; revision received 7 November 2001; accepted for publication 28 December 2001.

*Professor, Mechanical Engineering Department. Associate Fellow AIAA.
†Research Scientist, Mechanical Engineering Department.
‡Research Assistant; currently Engineer, Research and Development Engineering, Waters Corp., Milford, MA 01757.
§Professor, Mechanical Engineering Department. Senior Member AIAA.

For steady, turbulent diffusion flames, the strength of an air coflow can potentially have a noticeable effect on the flame length.[17,18] As the strength of the coflow is increased, for a given jet velocity, the flame tends to spread more slowly,[17] and the length of the combustion zone can increase.[18] Dahm and Dibble,[19] in the context of the examination of coflow effects on flame blowout, related the growth and entrainment characteristics of turbulent jet diffusion flames with coflow to those of nonreacting jets. Using nonreacting jet data,[20] Dahm and Dibble[19] illustrated that steady flames become more wakelike with increasing coflow, leading to a slower rate of flame spreading. The degree to which coflow impacts the flame length and structure of unsteady, turbulent diffusion flames under fully modulated conditions is the focus of the work described in this paper.

Experimental Description

Apparatus

The experimental setup consisted of a single fuel nozzle centered in a square duct (20 × 20 cm in cross section) through which coflow air was supplied, as shown schematically in Fig. 1. For some experiments, the coflow duct was removed and a flat plate was mounted 5.3 cm below the jet nozzle exit. This resulted in a free flame condition, where the fuel jet was discharged into still laboratory air. In this case, the flame was surrounded by a square screen enclosure 1.07 m on a side. The fuel gas nozzle consisted of a stainless steel tube with an inner diameter of $d = 2$ mm and a length to diameter ratio of 38. The coflow duct was 67 cm in length with walls of glass plate to allow for flow visualization. A honeycomb and two perforated plates were situated upstream of the injection nozzle, as shown in Fig. 1, with the distance between the nozzle and the top surface of the honeycomb of 4.1 cm. Laser Doppler velocimetry (LDV) surveys of the coflow indicated a wake velocity defect of 25% in the immediate vicinity of the nozzle and with a turbulence level of less than 5% at a location 2 cm downstream of the nozzle exit. The accuracy of the LDV measurements was approximately 0.5%, based on the number of data points taken (1000) and the rms value of the fluctuations in the wake region. Because the jet exit velocity exceeded the coflow velocity in all cases by a factor of at least 50, it is not believed that the coflow turbulence level had a significant effect on the behavior of the flames. An electrically heated Kanthal® wire of 0.28-mm diam situated within one nozzle diameter of the nozzle exit served as a continuous ignition source. The wire was approximately 10 mm in span and included a single loop roughly 4 mm in diameter parallel to the nozzle exit plane.

A fast-response solenoid valve (Parker Hannifin Series 9) was used to modulate the fuel flow. The opening/closing time of the valve

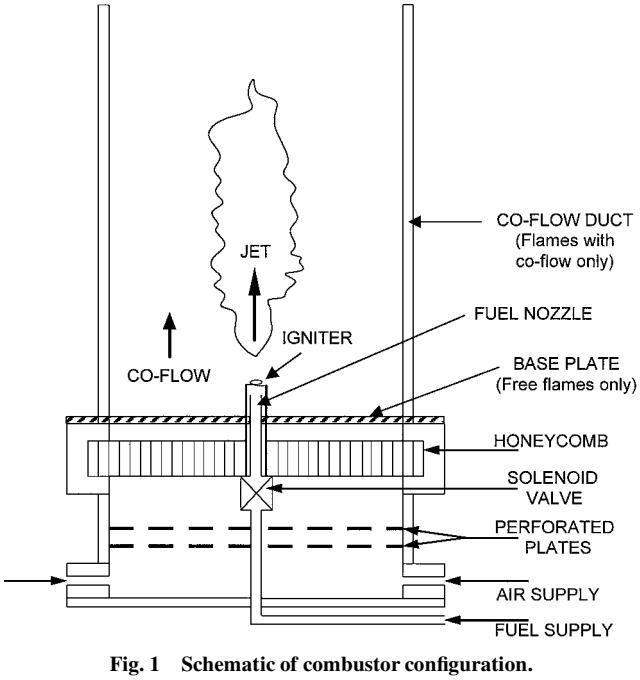

Fig. 1 Schematic of combustor configuration.

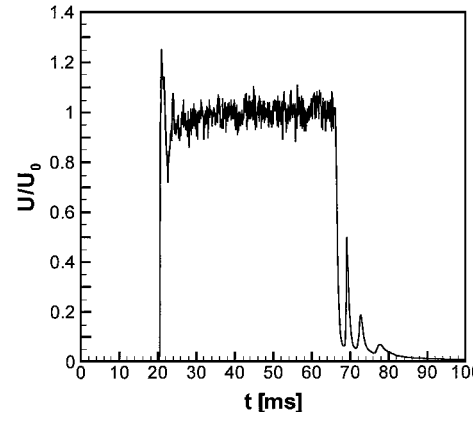

$\tau = 46$ ms

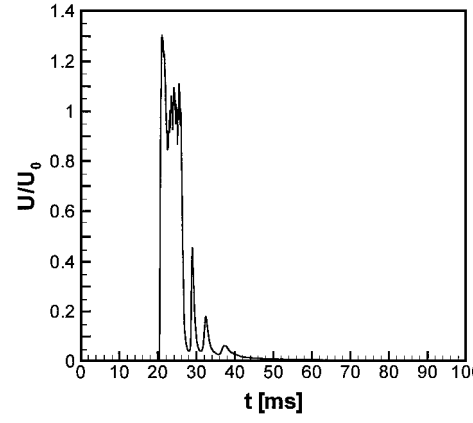

$\tau = 5.7$ ms

Fig. 2 Typical injection gas velocity cycle, test gas air, and no coflow.

was approximately 500 μs. In all cases, the jet was fully pulsed, that is, 100% modulated, at frequencies of up to 4 Hz. The valve opening and closing was controlled in an on–off (square-wave) fashion by a Parker Hannifin Iota One control unit. The actual gas velocity during the injection interval was somewhat different from a square wave largely due to the hydraulic response of the system. Sample time traces of the instantaneous jet exit velocity U normalized by the measured velocity averaged over the pulse, U_0, are shown in Fig. 2 for two different injection times. These data were taken using a hot wire placed immediately downstream of the nozzle exit. The accuracy of the hot-wire data was better than 2%, based on the rms value of the fluctuations observed during the steady portion of the injection interval combined with the uncertainty in the calibration.

The velocity traces typically indicate that there is a certain amount of velocity overshoot at the beginning of each pulse and that the trailing end of each pulse was often accompanied by flow oscillations. For the injection time of $\tau = 46$ ms, a reasonable approximation to the desired square-wave injection velocity profile was achieved. For injection times of 6 ms or longer, the injected volume associated with the overshoot and oscillations amounted to not more than 3% of the total. The hot-wire data also indicate that the average velocity during injection was not greatly impacted by the duration of the injection interval. The span of the hot wire actually exceeded the diameter of the jet nozzle exit, so that the measured velocity was somewhat lower than the actual mean bulk value. The actual value of the bulk jet injection velocity was determined using an Omega mass flow meter (Model FMA 824) under steady flow conditions. The jet velocity was accurate to 1.5%, based on the stated accuracy of the flow meter.

The fuel was ethylene, and both the fuel gas and the air coflow were unheated ($T \approx 300$ K). Ethylene fuel was chosen for its easy ignitability and for comparison with previous results. All experiments were conducted at atmospheric pressure.

The luminous flame emission was recorded visually using a Panasonic Model WV-650CP color charge-coupled device camera with a framing rate of 30 frames/s. In some cases, each video image was

digitally separated into two fields to give an effective framing rate of 60 frames/s. The luminous portion of the flames corresponded to the presence of soot particles, which, in turn, can be roughly associated with the local reaction surfaces.[21] The images were used to examine qualitatively the flame structure and to determine quantitatively the flame length by identifying and locating the most extreme downstream parcel of the luminous flame in the last image frame before the flame disappears. For the fully modulated flames, determining the flame length in this manner is relatively more straightforward than in steady flames, where flame parcels become separated from the bulk flow in the flame tip region.[22] To determine an average value for flame length, typically 30–50 images were analyzed for each injection case. The mean flame length measurements were estimated to be accurate to within approximately ±5%, based on the measurement uncertainty and the 95% confidence limit based on the maximum rms value of the flame length fluctuations.

Flow Conditions

The typical injection Reynolds number, based on the bulk velocity of the jet during the injection interval ($U_{\text{jet}} = 22.6$ m/s), the cold fuel viscosity, and the exit nozzle diameter, was $Re_{\text{jet}} = 5 \times 10^3$. A few tests were also run with $Re_{\text{jet}} = 3 \times 10^3$ ($U_{\text{jet}} = 13.6$ m/s). The injection times ranged from 5.7 to 303 ms. The wait time between injected puffs can be expressed in terms of the duty cycle (the jet-on fraction of each cycle) α. The duty cycle is the product of the injection frequency and the injection time. This implies, for example, that increasing the frequency for a fixed injection time leads to an increase in the value of the duty cycle. The duty cycle in this investigation ranged from $\alpha = 0.02$ for the shortest injection time ($\tau = 5.7$ ms) to $\alpha = 0.5$ for the longest ($\tau = 303$ ms). This was sufficiently short, for all cases in this study, to ensure that each puff completely burned out (as indicated visually) before the next puff was injected.[14,15] Therefore the duty cycle, being sufficiently short to give isolated puffs, is not a key parameter in the current study.

The injection frequency varied from 1.7 to 3.9 Hz. (These frequencies correspond to the injection times and duty-cycle limitation given earlier.) The corresponding Strouhal number, $Sr = fd/U_{\text{jet}}$, ranged from 1.5×10^{-4} to 3.5×10^{-4}. These values are far below the value of Strouhal number corresponding to the natural instability in the near-field region of the jet,[5,8] which is approximately $Sr = 0.25$.

The very short injection time and the small nozzle resulted in a small volume of fuel in each injected puff, ranging from $V_0 = 21.2$ cm^3 for the longest injection time ($\tau = 303$ ms) to $V_0 = 0.40$ cm^3 for the shortest ($\tau = 5.7$ ms). Coflow air was supplied to the combustor at a velocity of up to $U_{\text{cof}} = 45.7$ cm/s to give a ratio of the coflow velocity to that of the jet, $U_{\text{cof}}/U_{\text{jet}}$, ranging from 0 to 0.02. For the case where the coflow duct was in place but no coflow air supplied, the air required for combustion was drawn in through the combustor exit.

An important consideration in the case of fully modulated diffusion flames is whether the flow is driven primarily by buoyancy or by momentum. The scaling law for the velocity decay in buoyancy-driven cases differs significantly from the momentum-driven case, even in the limit of small heat release. The criterion developed by Becker and Yamazaki[23] states that, if the value of the parameter $\xi_L = (\rho_a dg/\rho_{\text{jet}} U_{\text{jet}}^2)^{1/3}(L/d)$ for a steady diffusion flame is less than approximately 2, the flame is considered to be momentum driven and when it is greater than roughly 10, it is considered to be buoyancy driven. Here ρ_a and ρ_{jet} are the density of the coflow and the jet gas, respectively, g is the gravitational acceleration, L is the flame length, and d is the jet nozzle diameter. For the steady flames in the present experiments, $\xi_L \approx 8.4$, thus indicating that the steady flames are likely primarily buoyancy driven. This argument would not necessarily be expected to hold for fully modulated flames. It has been suggested[15] that, in these flames, if anything, the transition to momentum-dominated flow would require significantly lower values than $\xi_L = 2$ because of the loss of jet momentum due to the rapid entrainment and mixing of ambient air that occurs for widely spaced puffs. Similar reasoning suggests that the transition to the fully buoyancy-dominated regime is complete for values of ξ_L less than 10. Alternatively, a global Richardson number can be determined based on the average buoyancy within the puff (from temperature measurements), the puff diameter, and the puff celerity. Both for the current study and for fully modulated puffs in an earlier study,[15] the resulting values of the Richardson number were around unity, indicative of the puffs being fully buoyancy driven. Therefore, we expect that the majority of the flames considered in this study were buoyancy driven.

Results

Flame Structure

Images of four representative flames (one steady and three fully modulated) are shown in Fig. 3 for the case where the coflow duct was present and with a normalized coflow velocity of $U_{\text{cof}}/U_{\text{jet}} = 0.005$. The vertical extent of all images is 58.4 cm. Figure 3a shows a steady turbulent flame; Figs. 3b–3d show fully modulated flames, each with a different injection time. Each fully modulated flame image shown is within one video field (17 ms) of the end of the injection interval. The steady flame exhibits the well-known fluctuations in flame length due to the burnout of large flame structures.[22] For the relatively long injection time ($\tau = 119$ ms) corresponding to Fig. 3b, an elongated flame structure is produced. In this case, the flame is generally similar in appearance to the steady-state flame, except for the flame tip region, which shows a pufflike cap structure that does not lead to the fluctuations in flame length seen in steady flames. The burnout length of these flames is comparable to those for steady flames. For shorter injection times (and smaller injection volumes), the flame length becomes noticeably shorter than that of the steady flame (Figs. 3c and 3d). Figure 3c shows an image near the end of the injection period of $\tau = 46$ ms. In this case, a pufflike structure is apparent in the region of the flame near the flame tip, with a tail attached to the trailing portion of the burning structure. These observations are similar to those reported previously for free flames.[15]

Changes in the structure of a typical fully modulated flame puff are apparent in the time sequence shown in Fig. 4 for an injection time of $\tau = 46$ ms. The time between each of the representative images shown is 17 ms, the first image is approximately 45 ms after pulse initiation, with the third image corresponding to the time just before the end of the injection interval. After the end of the injection period, the tail region is the first to disappear (fourth image). Subsequently, the vortexlike structure of the burning puff becomes more evident (sixth and seventh images), with the regions associated with the vortex cores generally being the last to be completely reacted as the time of combustion completion is approached (last image).

Although it may be tempting to relate the observations of the caplike structure at the leading edge of the fully modulated flames to the starting vortex formation seen in pulsed, nonreacting jets, there are major differences between the burning and isothermal cases. Formation of the starting vortex ring in free, isothermal jets has recently been investigated.[24] Such a starting vortex pinches off from the trailing jet close to the nozzle, and the resulting ring attains a circulation equivalent to that created by the first $4d$ long slug of injected fluid. Even with the shortest injection time considered in this work, the equivalent injected slug length is $64d$. Moreover, the diameter of a starting vortex scales with the nozzle diameter in the isothermal case, whereas in the fully modulated flame considered here, the lateral width of the puff, δ, is significantly greater than d (Fig. 5). Finally, separation of the puff from the burning stem is not observed for the fully modulated flames due to the acceleration of the flow structures brought by buoyancy. In the isothermal case, buoyant acceleration is absent, and the separation of the starting ring from the ensuing jet is quite apparent.[24,25]

The transition from compact pufflike to elongated flame behavior can be characterized in terms of the parameter

$$P \equiv (H/d)^{\frac{1}{3}} = (4V_0/\pi)^{\frac{1}{3}}/d = (U_{\text{jet}}\tau/d)^{\frac{1}{3}} \qquad (1)$$

This parameter was developed[15] by regarding the volume of injected gas as a cylinder of identical volume with a base diameter equal to the nozzle diameter d. The height of this cylinder, H, thus, is the total volume of injected gas divided by the nozzle exit area. The aspect ratio of this volume, H/d, can reasonably be expected to be related to whether a fully modulated flame puff will be compact

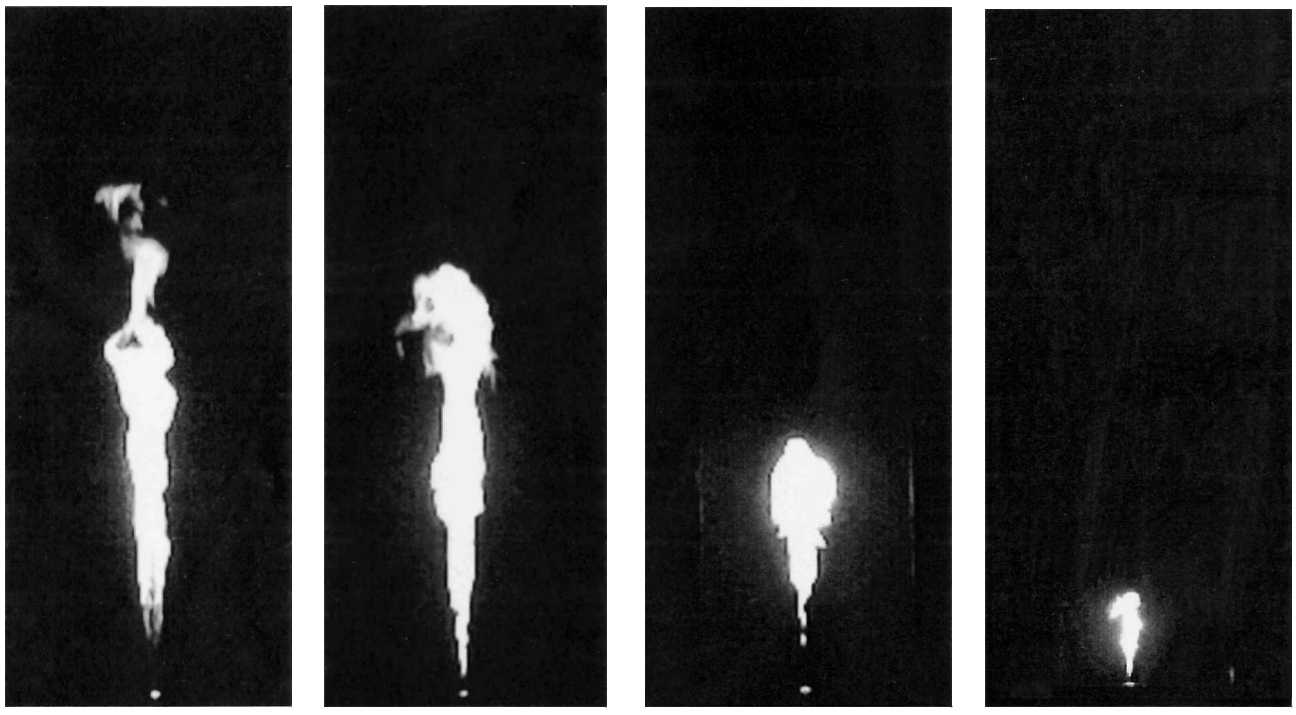

Fig. 3 Turbulent ethylene/air diffusion flames with low coflow, $Re_{jet} = 5 \times 10^3$, $U_{cof}/U_{jet} = 0.005$: a) steady flame; b) fully modulated flame with injection time $\tau = 119$ ms, injection volume $V_0 = 8.4$ cm^3, and duty cycle $\alpha = 0.32$; c) fully modulated flame with $\tau = 46$ ms, $V_0 = 3.2$ cm^3, and $\alpha = 0.15$; and d) fully modulated flame with $\tau = 5.7$ ms, $V_0 = 0.40$ cm^3, and $\alpha = 0.022$.

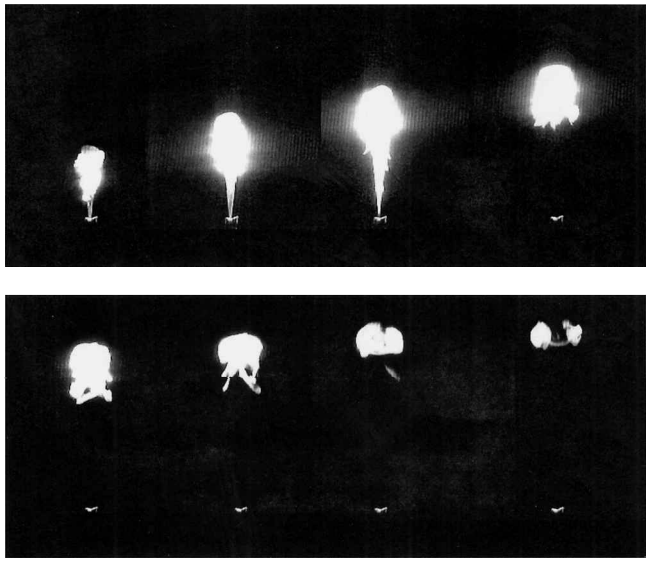

Fig. 4 Sequence of images for a fully modulated flame, $P = 8$, $\tau = 46$ ms, and $\alpha = 0.15$. The sequence proceeds from top left to bottom right.

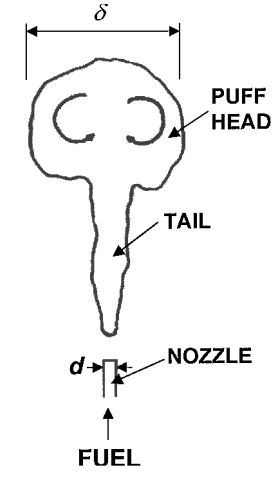

Fig. 5 Fully modulated flame puff near the end of the injection interval.

or more elongated in structure. When the visual description of the pulsed flames is compared with their characteristic P value, it is possible to correlate elongated structures with large values of P (long cylinders) and pufflike structures with small values of P (flat cylinders). Generally, pufflike behavior is seen for values of P not exceeding approximately $P = 8$ for ethylene/air flames. (The flame puff sequence shown in Fig. 4 is for this value of P.) In addition, for isolated, pufflike structures, the parameter P is directly related to the mean flame length because the latter has been shown previously[14,15] to scale with the cube root of the injected volume as follows:

$$L/d \sim P(1+\psi)^{\frac{1}{3}} \tag{2}$$

where ψ is the stoichiometric air/fuel ratio. The values of the injection parameter for the fully modulated flames shown in Figs. 3b–3d are $P = 11$, $P = 8$, and $P = 4$, respectively. For a given mean flow velocity and nozzle diameter, the injection parameter P is directly dependent on the injection time τ, as seen in Eq. (1).

Representative pairs of images of fully modulated flame puffs for three different coflow conditions are shown in Fig. 6a–6f. In this case, the injection parameter is $P = 8$ ($\tau = 46$ ms) and the time between images is 50 ms. The vertical extent of the images is 35 cm. The first pair of images, Figs. 6a and 6b, shows a fully modulated flame in the combustor with no coflow supplied. In this case, the necessary air for combustion was drawn in through the exit of the coflow duct. The fully modulated flame portrayed in the second image pair, Figs. 6c and 6d, had a coflow strength of $U_{cof}/U_{jet} = 0.005$. For these injection conditions, there does not appear to be a significant change in the flame structure due to the presence of the coflow. It would be reasonable to expect that the presence of coflow would cause some increase in the flame length; the amount of this increase is quantified in the next section. Finally, the free flame (no coflow

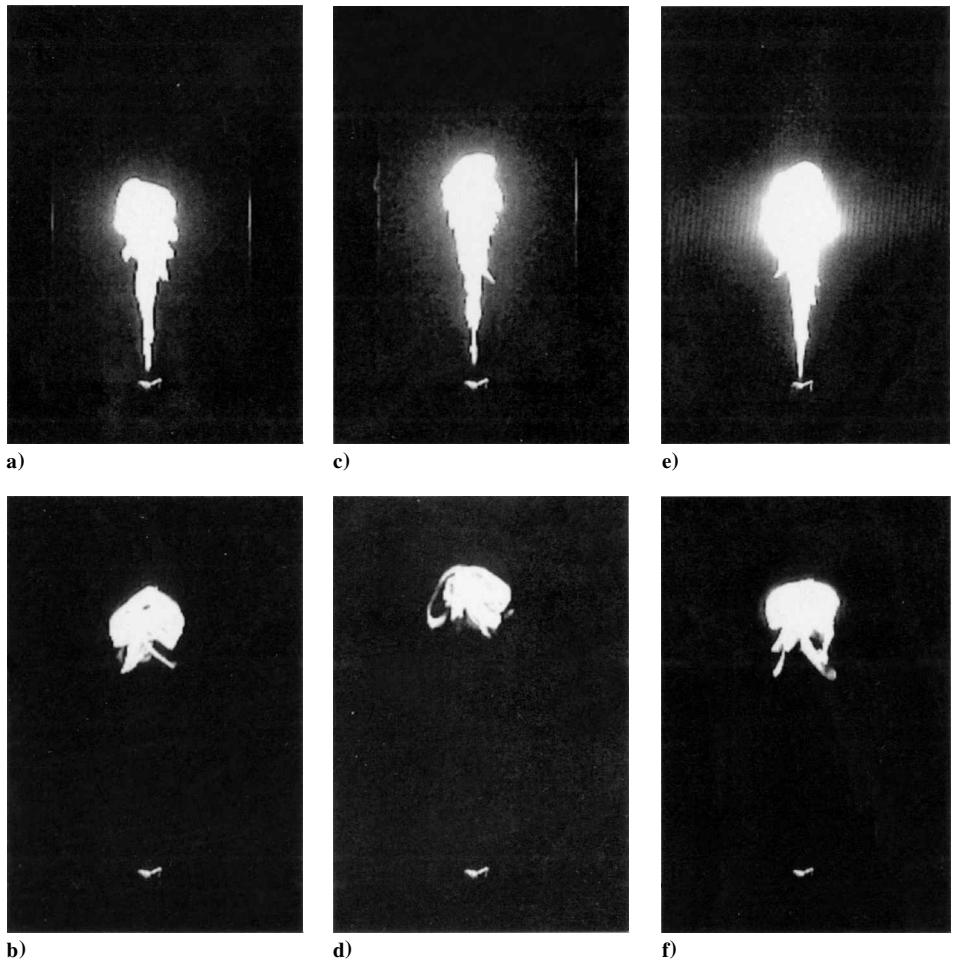

Fig. 6 Fully modulated, turbulent diffusion flames for $Re_{jet} = 5 \times 10^3$, $P = 8$ at $\tau = 46$ ms: a) ducted flame without coflow, first image; b) ducted flame without coflow, second image 50 ms after first; c) ducted flame with coflow of strength $U_{cof}/U_{jet} = 0.01$, first image; d) ducted flame with coflow of strength $U_{cof}/U_{jet} = 0.01$, second image 50 ms after first; e) free flame, first image; and f) free flame, second image 50 ms after first.

duct attached) for the same injection conditions is shown in Figs. 6e and 6f. The free flame appears generally similar in structure to the flames with the coflow duct (Figs. 6a and 6b). For steady flames, the addition of coflow for the range of velocities employed here appeared to have relatively little effect on the flame, both in terms of the mean flame length and flame structure. There was a slight narrowing of the flame accompanied by a small increase in mean flame length with increasing coflow.

Note that the images presented here are only representative images for each of the fully modulated flame and coflow conditions shown. To determine quantitatively the changes in flame length brought about by coflow, multiple images were considered, for which a mean flame length for each flow condition was determined. The results of that analysis are presented in the following section.

Mean Flame Length

The average measured flame length, normalized by the nozzle diameter, is shown in Fig. 7 for fully modulated flames with various coflow strengths and a Reynolds number of 5×10^3. The case of the free flame, which has no coflow and no duct, is included as a special case. The abscissa parameter [identified in Eq. (2)] allows comparison between fully modulated experiments using different fuel gases, specifically the natural gas cases shown in Fig. 7. For ethylene, $\psi = 14.3$ so that $P(1+\psi)^{1/3} = 2.48P = 2.48(U_{jet}\tau/d)^{1/3}$ for the current study.

For values of the injection parameter of up to approximately $P = 11$ [corresponding to $P(1+\psi)^{1/3} \approx 28$], the normalized flame length data appear to be reasonably consistent with the linear scaling with the parameter $P(1+\psi)^{1/3}$, even though the flames for $P > 8$ are not necessarily pufflike in appearance. For $P = 11$ [$P(1+\psi)^{1/3} = 28$], the normalized flame length appears to approach the steady-state value. The trends in normalized flame length of the current results, for both the free flames and the ducted flames, with and without coflow, are in reasonable agreement with previous results[15] for free flames. These data in fact suggest that, for a sufficiently large injected volume, the flame length of fully modulated flames reaches a value independent of the injection volume. (For sufficiently long injection time, the flame length would be expected

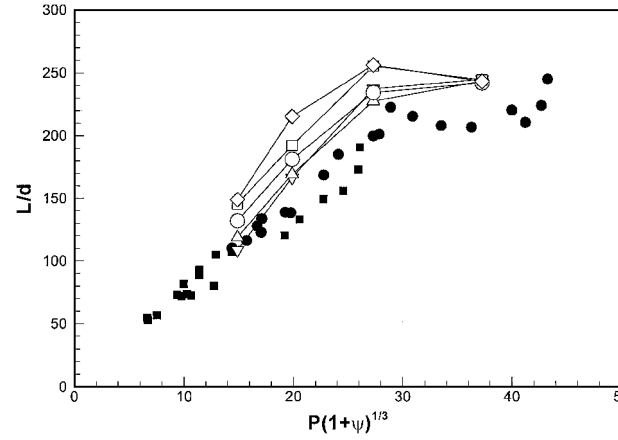

Fig. 7 Normalized flame length for isolated, fully modulated flame puffs for $Re_{jet} = 5 \times 10^3$: ▽, free flames; △, ducted flames with $U_{cof}/U_{jet} = 0$; ○, $U_{cof}/U_{jet} = 0.005$; □, $U_{cof}/U_{jet} = 0.01$; ◇, $U_{cof}/U_{jet} = 0.02$. Free flames of Hermanson et al.[15]: $Re_{jet} = 3.15 \times 10^3$–$2 \times 10^4$, $\alpha < 0.2$; ■, natural gas; and ●, ethylene.

to approach the corresponding flame length for a steady flame.) The average normalized steady-state flame length was $L/d \approx 240$.

For the pufflike flames [$P \leq 8$, $P(1+\psi)^{1/3} \leq 20$] the mean normalized flame length monotonically increases as the strength of the coflow increases, as can be seen in Fig. 7. The mean flame lengths of the ducted flames without coflow generally exceed slightly those of the corresponding free flames. Thus, it appears that, for the injection conditions of this study, there is no coflow strength, which gives the same mean flame length for a ducted flame as observed for the free flame.

On a fractional basis, the increase in flame length was 25% for $P = 6$ [$P(1+\psi)^{1/3} = 15$] as the coflow strength increased from zero to $U_{\text{cof}}/U_{\text{jet}} = 0.02$. The amount of flame length increase was comparable for the $P = 8$ case, amounting to approximately 27%. For values of P in excess of $P = 8$, the sensitivity of the flame length, on a fractional basis, decreased substantially. For $P = 11$ [$P(1+\psi)^{1/3} = 27$], the mean flame length increased no more than 13% for $U_{\text{cof}}/U_{\text{jet}} = 0.02$ compared with the case without coflow. The corresponding fractional impact of coflow for $P = 15$ [$P(1+\psi)^{1/3} = 37$] was much less, amounting to no more than 1%. (This was within the uncertainty of the measurement.) Thus, as the P value increases and more elongated flames result, the sensitivity of the mean flame length to coflow decreases markedly, leading to essentially no impact on flame length for $P > 11$. The mean steady-state flame length for the maximum coflow strength of $U_{\text{cof}}/U_{\text{jet}} = 0.02$ was within 4% (again, within the measurement uncertainty) of that of both the steady-state flame with no coflow and the corresponding free flame. For the case of $P = 4$, the imaging rate was not sufficiently high to allow for the reliable determination of the mean flame length.

The trends in normalized mean flame length vs the coflow strength for several fully modulated flames are shown in Fig. 8. The data for the free flames are shown for reference on the ordinate of Fig. 8. For the highest values of P ($P \geq 11$), as well as for the steady flame, essentially no systematic change in flame length with increasing coflow was apparent for the range of coflow strengths provided. (The $P = 15$ case is shown in Fig. 8). The sensitivity to coflow of fully modulated flames with values of the pulsing parameter $P \leq 8$ is apparent in Fig. 8. The mean flame length evidently increases with the addition of even the smallest amount of coflow employed here, $U_{\text{cof}}/U_{\text{jet}} = 0.001$. Note that there is necessarily a fundamental change in the flowfield in going from no coflow to even a very weak coflow. In the case with coflow, the airflow throughout the combustor, including the region near the fuel nozzle exit, has an axial component in the direction of fuel flow. This is not the case for the flame without coflow (in which case the fresh airflow at the combustor exit is in the opposite direction to the fuel flow) or for the free flame. The significance of changes in mean flame length for compact flame puffs in switching between the different flow regimes is unclear at present.

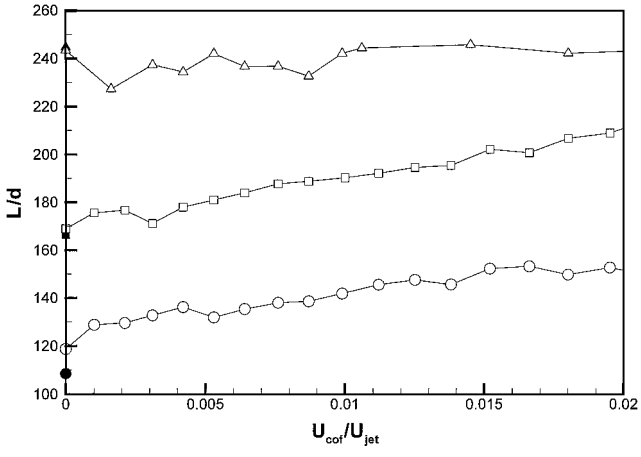

Fig. 8 Effect of coflow strength on normalized flame length for several values of injection parameter for $Re_{\text{jet}} = 5 \times 10^3$, ○, ●, $P = 6$; □, ■, $P = 8$; and △, ▲, $P = 15$. Solid symbols, free flames and open symbols, ducted flames with coflow.

Scaling Argument for Coflow Effects

To determine a characteristic value of coflow strength for a given increase in flame length for the widely separated puffs considered here, an argument based on the relative strength of the coflow and the puff core velocity may be invoked. It is hypothesized that the degree to which the coflow velocity affects the mean flame length depends on the strength of the coflow relative to an appropriate characteristic velocity for the burning fuel puff. A given change in the mean flame length is then expected for $U_{\text{cof}} = U_{\text{cl}}/k$, where U_{cl} is the centerline velocity of the gas in the puff and $k > 1$ is a constant to be determined from experimental data. To continue this argument, scaling laws for the puff celerity, s, and the puff centerline velocity U_{cl} are required. For isothermal buoyant puffs in the Boussinesq limit,

$$s \approx 2.8F^{\frac{1}{2}}z^{-1} \tag{3}$$

where z is the vertical distance from the source and F is the total buoyancy of the puff given by $F = g[(\rho_a - \rho_{\text{puff}})/\rho_a]V$. (Here, ρ_{puff} and ρ_a are, respectively, the average puff density and the ambient density.) The volume of the burning puff, V, is much larger than the injected fuel volume due to heat release and air entrainment. In the Boussinesq limit in a uniform, isothermal environment, F is conserved, whereas in pufflike diffusion flames, F varies due to the heat release and the accompanying density changes. Previous experiments[15] have shown that the celerity of diffusion flame puffs in the region near the mean flame length is approximately similar to that of isothermal puffs, but with a different constant:

$$s \approx 6.2F^{\frac{1}{2}}z^{-1} \tag{4}$$

The centerline gas velocity is roughly twice the celerity,[26,27] so that

$$U_{\text{cl}} \approx 2\left(6.2F^{\frac{1}{2}}z^{-1}\right) \tag{5}$$

The density ratio in the expression for F can be found from the temperatures in the puff and the coflow air assuming uniform pressure. Moreover, the puff volume increases as its radius cubed, $V \approx 3r^3$, with the proportionality constant of 3 taken from previous isothermal experiments.[28] Strictly speaking, the coflow velocity would likely enter the scaling of puff width with downstream distance; this minor effect is not being considered here. It could also be pointed out that, after burnout, the visible puff size is zero. However, in this case, the scaling argument regarding coflow effects is no longer relevant.

On dimensional grounds, the puff radius r must scale with the distance z from the source in the far field of turbulent puffs. Examination of sequences of burning puffs (such as Fig. 4) indicates that up to the point of puff burnout, the puff diameter increases with distance as roughly $r \approx 0.16z$. Thus, F can be estimated for pufflike diffusion flames based on this scaling relationship to get

$$F \approx g(1 - T_a/T_{\text{puff}})(0.012z^3) \tag{5}$$

Subsequently, the puff centerline velocity is

$$U_{\text{cl}} \approx 1.4[g(1 - T_a/T_{\text{puff}})z]^{\frac{1}{2}} = 1.4\,[g'(z)z]^{\frac{1}{2}} \tag{6}$$

where $g' = g(1 - T_a/T_{\text{puff}})$ and T_{puff} and T_a is the mean temperature near the flame tip and the temperature of the coflow, respectively. Requiring that the coflow velocity be a fraction of the puff centerline velocity at the flame tip, $z = L$, allows determination of the coflow velocity for a given increase in mean flame length:

$$U_{\text{cof}} < U_{\text{cl}}(z = L)/k \approx 1.4[g'(z = L)L]^{\frac{1}{2}}/k \tag{7}$$

Finally, expression (7) can be nondimensionalized by the velocity at the source, U_{jet}, to give

$$\left.\frac{U_{\text{cof}}}{U_{\text{jet}}}\right)_{\text{char}} = \frac{1.4}{k}\left[g'(z = L)\frac{L}{U_{\text{jet}}^2}\right]^{\frac{1}{2}} \tag{8}$$

Thus, the characteristic value of $U_{\text{cof}}/U_{\text{jet}}$ depends on the flame length, the average temperature at the flame tip, and the jet source

velocity. The mean flame length L of widely separated puffs is, thus, expected to scale linearly with P (and, hence, the injection time), as discussed earlier, so that $L/d = a(1+\psi)^{1/3}P$, where a is an empirically determined constant. This scaling assumes that the flame length asymptotes to zero in the limit of $P = 0$ (zero injected fuel volume). The current mean flame length results for $6 \le P \le 11$ suggest the value $a = 9.84$ for a coflow strength of $U_{\text{cof}}/U_{\text{jet}} = 0.01$. Temperature measurements in previous experiments[15] with isolated fully modulated diffusion flame puffs have indicated that the mean puff temperatures near the flame tip are generally around $T_{\text{puff}} = 400°\text{C}$, regardless of the puff injection conditions. This temperature is an average in the puff region, where there has been substantial entrainment of excess air, and is not representative of a flame sheet or stoichiometric surface. Substituting for L/d then allows the direct determination of the expected characteristic coflow velocity as a function of injection conditions for a given fuel:

$$\left(\frac{U_{\text{cof}}}{U_{\text{jet}}}\right)_{\text{char}} = \frac{4.3}{k}\left[\frac{gd}{U_{\text{jet}}^2}\left(1-\frac{T_a}{T_{\text{puff}}}\right)(1+\psi)^{\frac{1}{3}}P\right]^{\frac{1}{2}}$$

$$= \frac{4.3}{k}\left[\frac{gd^{\frac{2}{3}}}{U_{\text{jet}}^{\frac{5}{3}}}\left(1-\frac{T_a}{T_{\text{puff}}}\right)(1+\psi)^{\frac{1}{3}}\tau^{\frac{1}{3}}\right]^{\frac{1}{2}} \tag{9}$$

The utility of the preceding argument in determining a threshold for the onset of coflow effects in fully modulated, turbulent, diffusion flames can be determined from a systematic examination of the mean flame length for the full range of coflow strengths employed in this investigation. The observed coflow strength required to produce a given increase in mean flame length are compared with the predicted values of the characteristic coflow strength in Fig. 9. The data points shown correspond to an increase in the mean flame length of 15%, with the upper and lower bars corresponding to flame length changes of 18 and 12%, respectively. The curves, for two values of Reynolds number, were generated for ethylene fuel using the scaling arguments developed earlier [Eq. (9)]. The experimentally determined values of the characteristic coflow velocity are seen to be in reasonable agreement with those suggested by the scaling argument for a value of $k = 8.9$. The value of this constant would naturally be different for a different fractional change in mean flame length than the 15% chosen here.

Though the choice of a 15% increase in mean flame length as a threshold value is rather arbitrary, the experimental results shown in Fig. 9 lend support to the two essential predictions of the scaling argument developed here, that is, that the amount of coflow required to achieve a given increase in the mean flame length 1) increases as the injection time, that is, P, is increased, for a given Reynolds number and 2) decreases for a given injection time (or P) with increasing Reynolds number. For a fixed value of both the injection parameter P and the coflow strength, no systematic dependence of the flame length on Reynolds number was observed.

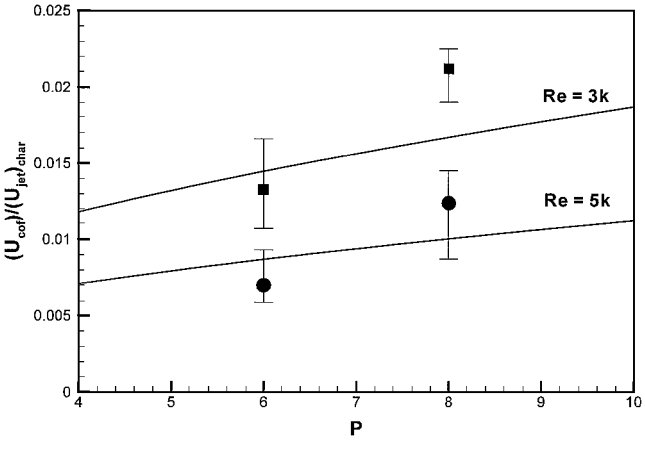

Fig. 9 Predicted characteristic coflow strength corresponding to a 15% increase in mean flame length: solid curves, analytical result; experimental results (from Fig. 8): ●, $Re = 5 \times 10^3$; and ■, $Re = 3 \times 10^3$.

Note that the proposed scaling argument is only expected to be valid for compact, pufflike structures, which require a value of $P \le 8$ for ethylene fuel. A threshold value of coflow strength for the more elongated structures corresponding to higher values of P is not yet established. (The coflow also appears to have a less marked impact on flame length in these cases.)

Summary

A pulsed fuel injector system was used to study the flame structure and flame length of fully modulated jet diffusion flames over a range of injection times with a variable air coflow. In all cases, the jet was completely shut off between pulses (fully modulated) for an interval sufficient to ensure widely spaced, noninteracting puffs. The fuel consisted of ethylene at 1-atm pressure. Imaging of the luminosity from the flame revealed distinct types of flame structure, depending on the length of the injection interval. For short injection times (small injected volume) and short duty cycle, pufflike flame structures were observed. The burnout length of the puffs was at least 51% less than the steady-state flame length. For relatively longer injection times, a more elongated shaped flame resulted. The mean flame lengths of the elongated flames were generally comparable to those of the corresponding steady-state cases. For compact puffs, the addition of coflow for ducted flames generally resulted in an increase in the flame length, amounting to an increase in flame length of up to 27% for a coflow strength of $U_{\text{cof}}/U_{\text{jet}} = 0.02$. The effect of coflow on the normalized flame length of pulsed flames with longer injection times, as well as steady flames, was much less. The mean flame length for flames in the ducted combustor generally exceeded that of the corresponding free flames, even for the case where no coflow air was supplied. A characteristic value for the coflow strength at which a specified change in flame length occurs is developed and is seen to be in good agreement with the experimental results.

Acknowledgments

This work was supported by the NASA Microgravity Research Division under Cooperative Agreement NCC3-673. The authors acknowledge helpful discussions with D. P. Stocker and with U. G. Hegde and the assistance of N. Demmons in conducting the experiments reported here.

References

[1]Tang, Y. M., Ku, S. H., Daniel, B. R., Jagoda, J. I., and Zinn, B. T., "Controlling the Rich Limit of Operation of Pulse Combustors," *Twenty-Third Symposium (International) on Combustion*, Combustion Inst., Pittsburgh, PA, 1995, pp. 1005–1010.

[2]Keller, J. O., and Hongo, I., "Pulse Combustion: The Mechanisms of NO_x Production," *Combustion and Flame*, Vol. 80, No. 3–4, 1990, pp. 219–237.

[3]Keller, J. O., and Westbrook, C. K., "Response of Pulse Combustor to Changes in Fuel Composition," *Twenty-First Symposium (International) on Combustion*, Combustion Inst., Pittsburgh, PA, 1986, pp. 547–555.

[4]Tang, Y. M., Waldherr, G., Jagoda, J. I., and Zinn, B. T., "Heat Release Timing in a Nonpremixed Helmholtz Pulse Combustor," *Combustion and Flame*, Vol. 100, No. 1–2, 1995, pp. 251–261.

[5]Crowe, S. C., and Champagne, F. H., "Orderly Structure in Jet Turbulence," *Journal of Fluid Mechanics*, Vol. 48, 1971, pp. 547–591.

[6]Long, D. F., Kim, H., and Arndt, R. E. A., "Controlled Suppression or Amplification of Turbulent Jet Noise," *AIAA Journal*, Vol. 23, No. 6, 1985, pp. 828–833.

[7]Bremhorst, K., and Hollis, P. G., "Velocity Field of an Axisymmetric Pulsed, Subsonic Air Jet," *AIAA Journal*, Vol. 28, No. 12, 1990, pp. 2043–2049.

[8]Vermeulen, P. J., Ramesh, V., and Yu, W. K., "Measurement of Entrainment by Acoustically Pulsed Axisymmetric Air Jets," *Journal of Engineering for Gas Turbines and Power*, Vol. 108, No. 3, 1986, pp. 479–484.

[9]Lovett, J. A., and Turns, S. R., "Experiments on Axisymmetrically Pulsed Turbulent Jet Flames," *AIAA Journal*, Vol. 28, No. 1, 1990, pp. 38–46.

[10]Reuter, D. M., Hedge, U. G., and Zinn, B. T., "Flowfield Measurements in an Unstable Ramjet Burner," *Journal of Propulsion and Power*, Vol. 6, No. 6, 1990, pp. 680–865.

[11]Reuter, D. M., Daniel, B. R., Jagoda, J. I., and Zinn, B. T., "Periodic Mixing and Combustion Processes in Gas Fired Pulsating Combustors," *Combustion and Flame*, Vol. 65, No. 3, 1986, pp. 281–290.

[12]Chen, T. Y., Hegde, U. G., Daniel, B. R., and Zinn, B. T., "Flame Radiation and Acoustic Intensity Measurements in Acoustically Excited Diffusion Flames," *Journal of Propulsion and Power*, Vol. 9, No. 2, 1993, pp. 210–216.

[13]Hegde, U. G., Reuter, D. M., and Zinn, B. T., "Sound Generation by Ducted Flames," *AIAA Journal*, Vol. 26, No. 5, 1988, pp. 532–537.

[14]Johari, H., and Motevalli, V., "Flame Length Measurements of Burning Fuel Puffs," *Combustion Science and Technology*, Vol. 94, No. 1–6, 1993, pp. 229–245.

[15]Hermanson, J. C., Dugnani, R., and Johari, H., "Structure and Flame Length of Fully-Modulated Diffusion Flames," *Combustion Science and Technology*, Vol. 155, 2000, pp. 203–225.

[16]Jones, H. R. N., and Leng, J., "The Effect of Hydrogen and Propane Addition on the Operation of a Natural Gas-Fired Pulsed Combustor," *Combustion and Flame*, Vol. 99, No. 2, 1994, pp. 404–412.

[17]Montgomery, C. J., Kaplan, C. R., and Oran, E. S., "Effect of Coflow Velocity on a Lifted Methane–Air Jet Diffusion Flame," *Twenty-Seventh Symposium (International) on Combustion*, Combustion Inst., Pittsburgh, PA, 1998, pp. 1175–1182.

[18]Thring, M. W., and Newby, M. P., "Combustion Length of Enclosed Turbulent Jet Flames," *Fourth Symposium (International) on Combustion*, Combustion Inst., Pittsburgh, PA, 1953, pp. 789–796.

[19]Dahm, W. J. A., and Dibble, R. W., "Coflowing Turbulent Jet Diffusion Flame Blowout," *Twenty-Second Symposium (International) on Combustion*, Combustion Inst., Pittsburgh, PA, 1988, pp. 801–808.

[20]Biringen, S., "An Experimental Study of a Turbulent Axisymmetric Jet Issuing into a Coflowing Air Stream," von Kármán Inst., TN 110, Rhode Saint Genese, Belgium, 1975.

[21]Haynes, B. S., and Wagner, H. G., "Soot Formation," *Progress in Energy and Combustion Science*, Vol. 7, No. 4, 1981, pp. 229–273.

[22]Mungal, M. G., Karasso, P. S., and Lozano, A., "The Visible Structure of Turbulent Jet Diffusion Flames: Large-Scale Organization and Flame Tip Oscillation," *Combustion Science and Technology*, Vol. 76, No. 4–6, 1991, pp. 165–185.

[23]Becker, H. A., and Yamazaki, S., "Entrainment, Momentum Flux and Temperature in Vertical Free Turbulent Diffusion Flames," *Combustion and Flame*, Vol. 33, No. 2, 1978, pp. 123–149.

[24]Johari, H., Zhang, Q., Rose, M., and Bourque, S., "Impulsively Started Turbulent Jets," *AIAA Journal*, Vol. 35, No. 4, 1997, pp. 657–662.

[25]Gharib, M., Rambod, E., and Shariff, K., "A Universal Time Scale for Vortex Ring Formation," *Journal of Fluid Mechanics*, Vol. 360, 1998, pp. 121–140.

[26]Turner, J. S., "Buoyant Plumes and Thermals," *Annual Review of Fluid Mechanics*, Vol. 1, 1969, pp. 29–44.

[27]Turner, J. S., *Buoyancy Effects in Fluids*, Cambridge Univ. Press, Cambridge, England, U.K., 1973, pp. 186–189.

[28]Scorer, R. S., "Experiments on Convection of Isolated Masses of Buoyant Fluid," *Journal of Fluid Mechanics*, Vol. 2, 1962, pp. 583–594.

J. R. Bellan
Associate Editor